Journal of Translational Medicine

RESEARCH

Open Access

Taltirelin induces TH expression by regulating TRHR and RARα in medium spiny neurons

Kedong Zhu[1], Lanxia Meng[1], Jiaying Luo[1], Tingting Wen[1], Liang Dan[1], Zhihao Wang[1], Xuebing Cao[2], Zhaohui Zhang[1*] and Guiqin Chen[1*]

Abstract

Taltirelin, an orally effective thyrotropin-releasing hormone analog, significantly improves motor impairments in rat models of Parkinson's disease (PD) and enhances dopamine release within the striatum. However, the underlying mechanism remains unclear. In this study, a variety of in vivo and in vitro methods, including transcriptomic analysis, were employed to elucidate the effects of Taltirelin on cellular composition and signaling pathways in the striatum of hemi-PD rats. We demonstrated that Taltirelin upregulates the expression of TRHR on striatal GABAergic neurons, which is accompanied by activation of the TRHR-MAPK-RARα-DRD2 pathway. Consequently, Taltirelin induces medium spiny neurons in the striatum to express TH. This discovery provides valuable insights into the potential application of Taltirelin in neurological disorders and offers new directions for drug development.

Keywords Taltirelin, Dopamine receptor D2, Tyrosine hydroxylase, Thyrotropin-releasing hormone receptor

Introduction

Thyrotropin-releasing hormone (TRH) is traditionally recognized as a neuroendocrine hormone synthesized in the hypothalamus that regulates the levels of thyroid-stimulating hormone and prolactin. Additionally, it plays a significant role in neurodegenerative diseases [1]. TRH can activate brain circuits, stimulate spinal motor neurons, and exhibit modulatory effects in various neurological disorders, such as spinocerebellar degeneration [2], amyotrophic lateral sclerosis [3], depression [4], Alzheimer's disease (AD) [5] and Parkinson's disease (PD) [6]. In the classic 6-OHDA PD model, TRH expression is significantly upregulated in the dopamine-depleted striatum [7]. Furthermore, L-DOPA treatment leads to a marked increase in the expression levels of TRH and tyrosine hydroxylase (TH) in the dopamine-depleted striatum of rats [7, 8]. Moreover, a single-cell study has demonstrated that a subset of interneurons expressing TH in the striatum also co-express TRH [9]. These findings suggest that TRH-related signaling cascades play a crucial role in the pathophysiology and potential treatment of Parkinson's disease. However, potent endocrine side effects limit its clinical utility [10].

Taltirelin(TAL), an orally effective TRH analog, possesses approximately 10–100 times stronger central nervous system stimulatory activity than TRH and a prolonged duration of action that is eight times longer [11]. Notably, it generates fewer endocrine side effects [12]. TAL has been approved for the treatment of

*Correspondence:
Zhaohui Zhang
zhzhqing1990@163.com
Guiqin Chen
chenguiqin@whu.edu.cn
[1] Department of Neurology, Renmin Hospital of Wuhan University, Wuhan 430060, Hubei, China
[2] Department of Neurology, Union Hospital, Tongji Medical College, , Huazhong University of Science and Technology, Wuhan 430022, Hubei, China

spinocerebellar degeneration, highlighting its tremendous potential in the field of neurology [13].

PD, the second most prevalent neurodegenerative disorder among elderly individuals, currently lacks a cure and often leads to severe disability and high mortality rates [14]. The characteristic symptoms of PD, including bradykinesia, tremor, and rigidity, are primarily attributed to the significant loss of dopaminergic neurons and subsequent dopamine(DA) deficiency [15]. DA replacement therapy with drugs such as levodopa (L-DOPA) remains the mainstay of treatment for PD [16]. However, long-term administration of L-DOPA can damage the remaining dopaminergic neurons [17] and is prone to induce motor complications and dose fluctuations [18, 19]. Consequently, there is an urgent need for the development of novel DA agonists. Our previous reports have revealed the neuroprotective effects of TAL on dopaminergic neurons, shielding them from the neurotoxicity induced by MPTP and rotenone [20]. Furthermore, TAL improves motor impairments in Hemi-PD Rats, along with the promotion of TH expression in the striatum [21], and significantly increases DA levels in the nucleus accumbens and dorsal striatum in normal rats [22]. However, the underlying mechanism remains unclear.

In the midbrain, the expression of TH has long been regarded as a hallmark for identifying dopaminergic neurons. However, in the striatum, this definition is more complex, as certain interneurons in the striatum have been found to express TH but appear to lack other enzymes or transporters necessary for typical dopaminergic neuronal function [23, 24]. The majority of neurons in the striatum are GABAergic medium spiny neurons (MSNs) that receive axonal projections from dopaminergic neurons of the substantia nigra, forming dopaminergic synapses [25]. Based on their expression of DA receptors (DRD2 and DRD1), MSNs can be divided into two subtypes: D1-MSNs, which primarily express substance P and dynorphin [26, 27], and D2-MSNs, which mainly express enkephalin [28]. Interestingly, study suggests that TRH receptor (TRHR) is differentially expressed across distinct regions of D2-MSNs in the striatum [29]. Furthermore, some specific subpopulations of D2-MSNs have been shown to express TH [23, 29]. Therefore, the mechanism by which TAL promotes sustained DA release in the striatum requires further investigation. In this report, we elucidate the anti-parkinsonian mechanisms of TAL in the striatum at the transcriptomic level. Moreover, in a PD animal model, we discovered that TAL regulates the expression of TRHR and retinoic acid receptor alpha (RARα), and induces medium spiny neurons in the striatum to express TH.

Materials and methods

Animals

Adult male Sprague–Dawley rats (48 in total, provided by Beijing HFK Bioscience Co., Ltd., China) weighing 230–250 g (7 weeks old) were used in this study. The animals were provided ad libitum access to food and water and maintained under a 12-h light/dark cycle with controlled temperature and humidity. Under the guidelines of the Institutional Animal Care and Use Committee (IACUC), efforts were made to minimize the number of animals used while maintaining consistent experimental conditions. This study was approved by the IACUC of Renmin Hospital of Wuhan University, ensuring compliance with animal welfare and ethical standards.

Stereotaxic surgery

For the Hemi-PD rats, animals were anesthetized with isoflurane gas and fixed onto a stereotaxic apparatus (RWD Life Science Co., Ltd., China). Body temperature was maintained at 37 °C using a temperature controller system. A total dose of 16 μg of 6-hydroxydopamine (Sigma, USA) was dissolved in 4 μL of sterile 0.9% saline solution containing 0.02% ascorbic acid. The solution was then injected into the right medial forebrain bundle at a rate of 0.5 μL/min using a 10 μL microsyringe. The coordinates for injection were as follows: anteroposterior, −4.4 mm; mediolateral, − 1.5 mm; dorsoventral, 7.8 mm from the dura [30]. After a 5-min dwell time, the microsyringe was slowly retracted. Behavioral evaluation of contralateral rotation induced by apomorphine was conducted 2 weeks after recovery.

Apomorphine-Induced rotation test and adjusting step test

At 2 weeks postsurgery, contralateral rotational behavior, indicative of dopaminergic lesion efficacy, was measured using a subthreshold dose of apomorphine (0.05 mg/kg, s.c.). Rats that exhibited more than 200 rotations toward the lesioned side within 30 min were considered to closely resemble a near-complete lesion model and were selected for further investigation [31]. To assess adjustment stepping in the gait test, the hindlimbs of the lesioned rats and the contralateral forelimb were gently lifted, leaving only the forelimb to touch the platform. The rats were then slowly moved along the runway at a speed of 90 cm within a 5-s interval. The number of adjusting steps in the forward direction for each forelimb was recorded three times and averaged to determine the stepping in the adjustment stepping test [32].

Treatment

The rats were administered treatment once daily. Successfully modeled hemi-PD rats were randomly divided

into two groups based on the treatment they received: the TAL group (N = 8), which received daily intraperitoneal injections of 5 mg/kg TAL, and the control (CTR, N = 8) group, which received an equivalent volume of saline. Thirty minutes after each injection of TAL or saline, the number of adjusting steps was assessed to evaluate the efficacy of TAL. After 7 days of injections, tissue samples were collected from both groups for further analysis, 30 min after the final injection of either TAL or saline.

Extraction of RNA from rat striatum

The rat striatum was collected and placed into corresponding labeled grinding tubes. Then, 1.5 mL of TRIzol lysis reagent was added to each tube, followed by grinding the tissue using a tissue homogenizer for 30 s. The tubes were removed and allowed to stand for 5 min to ensure sufficient cell lysis. After grinding and homogenization, the tissue samples were centrifuged at 4 °C and 12,000 g for 5 min. The supernatant was carefully transferred to new 1.5 mL centrifuge tubes and mixed with 300 µL of chloroform/isoamyl alcohol (24:1) by vigorous shaking. The tubes were then centrifuged at 4 °C and 12,000 × g for 8 min. The clear upper layer was transferred to new tubes, and 2/3 of the volume of the supernatant was mixed with isopropanol by gentle inversion. The tubes were then placed in a − 20 °C freezer and allowed to stand for at least 2 h. Subsequently, the tubes were centrifuged at 4 °C and 17,500 × g for 25 min, and the supernatant was discarded. The pellet was washed with 0.9 mL of 75% ethanol by gently suspending and inverting the tube. The tubes were then centrifuged at 4 °C and 17,500 × g for 3 min. The supernatant was discarded, and the remaining liquid was aspirated after brief centrifugation. The pellet was air-dried for 3–5 min and dissolved in 100 µL of RNase-free water.

mRNA library preparation

Each sample utilized 50 µL of RNA solution, undergoing mRNA enrichment, fragmentation, single-stranded cDNA synthesis, double-stranded cDNA synthesis, repair, and amplification to obtain single-stranded circular products. Linear DNA molecules that were not circularized were digested. The single-stranded circular DNA molecules were subjected to rolling-circle replication, resulting in DNA nanoballs containing multiple copies. The obtained DNA nanoballs were loaded into the nanopores of a high-density DNA nanochip using combinatorial probe-anchor synthesis technology for sequencing. The raw data obtained from sequencing were filtered using SOAPnuke software (v1.5.2) to obtain clean data [33]. The clean data were aligned to the reference gene sequences using Bowtie2 software (v2.2.5) [34], and the gene expression levels of each sample were calculated using the RESM software package (v1.2.8) [35]. Intragroup differential gene analysis was performed using DESeq with the condition of $|\log2FC| \geq 2$ and adjusted P-value < 0.05 [36]. The differentially expressed gene set was visualized using the heatmap function to generate a clustered heatmap. Based on the Gene Ontology (GO) and Kyoto Encyclopedia of Genes and Genomes (KEGG) annotation results and official classification, the differentially expressed genes (DEGs) were functionally classified. KEGG enrichment analysis was performed using the phyper function in the R software package, and GO enrichment analysis was performed using the TermFinder package. A threshold of q-value < 0.05 was used, and genes meeting this criterion were considered significantly enriched in the candidate gene set.

RT–PCR

Total mRNA was extracted from the striatum of each rat group using TRIzol reagent (Invitrogen). Complementary DNA synthesis was performed using the iScript cDNA Synthesis Kit (Bio-Rad). Quantitative PCR was conducted on a LightCycler 480 real-time PCR system (Roche) using LightCycler 480 SYBR Green 1 Master Mix. PCR begins at 94 °C for 5 min, followed by 40 cycles of 94 °C for 10 s, 60 °C for 20 s, and 72 °C for 15 s. Afterward, there is a final step of 94 °C for 30 s, 55 °C for 30 s, and 94 °C for 30 s. Amplification curves and melt curves are obtained, and PCR products are analyzed to confirm amplification specificity. The primer sequences are presented in.

SH-SY5Y neuroblastoma cell culture

SH-SY5Y cells were cultured in DMEM/F12 medium (HyClone, South Logan, UT, USA) supplemented with 10% FBS (Gibco, Carlsbad, CA, USA) and 100 units/ml penicillin–streptomycin. The cells were maintained in a humidified incubator at 37 °C with 5% CO2, and the culture medium was replaced every 3 days. Upon reaching 80% confluence, the cells were seeded onto appropriate multiwell plates at a density of 4×10^5 cells/ml. SH-SY5Y cells were then incubated with 5 µM TAL or an equal volume of PBS for 48 h, creating the TAL experimental group and the CTR control group. Besides, prior to treatment with 5 µM TAL for 24 h, SH-SY5Y cells were transfected with the Flag-His-TRHR plasmid or siRNA-TRHR to manipulate TRHR expression. The cells were then divided into five groups: CTR control group, knockdown (KD) group, overexpression (OE) group, KD + TAL group, and OE + TAL group.

Western blot analysis

Rat brain tissue was lysed in NP-40 lysis buffer supplemented with a protease inhibitor cocktail, followed by centrifugation at 15,000 rpm for 15 min at 4 °C. The

protein concentration in the supernatant was quantified using the BCA assay and subjected to Western blot analysis. After SDS–polyacrylamide gel electrophoresis, the proteins were transferred onto nitrocellulose membranes. The membranes were blocked with 5% skim milk for 1 h at 4 °C, followed by overnight incubation with the primary antibody. After washing the membranes three times with TBST, they were incubated with the secondary antibody for 1 h at room temperature. Following three additional washes with TBST, the signal was detected using an enhanced chemiluminescence method. Primary antibodies against the following targets were used: TH (Santa Cruz Biotechnology, sc-25269, 1:2000), TRHR (Novus Biologicals, NBP2-24726, 1:1000), ERK1/2 (Cell Signaling Technology, 4695 s, 1:4000), P-ERK1/2 (Cell Signaling Technology, 4370 s, 1:2000), GABA (Abcam, ab86186, 1:8000), RARα (ABclonal, A0370, 1:8000), DRD1 (Novus Biologicals, NB110-60017, 1:1000), DRD2 (ABclonal, A12930, 1:1000; Novus Biologicals, MAB9266, 1:1000), and GAPDH (Proteintech, 60,004–1-Ig, 1:8000).

Immunohistochemistry and immunofluorescence

After anesthesia, rat brains were perfused with cold PBS and 4% paraformaldehyde (PFA). The brains were then stored in 4% PFA at 4 °C for 24 h and subsequently embedded in paraffin. Serial 5 μm thick sections were prepared from each animal group and used for immunohistochemistry and immunofluorescence analyses. Paraffin-embedded rat brain sections were deparaffinized, rehydrated, and subjected to antigen retrieval by incubation in antigen retrieval buffer (0.1 M sodium citrate, pH 6.0) at 94 °C for 20 min. Endogenous peroxidase activity was blocked with 3% H2O2 for 10 min, followed by three washes in PBS. The sections were then blocked with 1% bovine serum albumin and 0.3% Triton X-100 in PBS for 30 min and subsequently incubated with the primary antibody overnight at 4 °C. After three washes in PBS containing 0.1% Triton-X 100, the immunohistochemistry signal was visualized using the Histostain-SP kit (Invitrogen). For immunofluorescence staining, the slides were incubated with secondary antibodies conjugated to Alexa Fluor 488 or Alexa Fluor 594. SH-SY5Y cells were fixed with 4% PFA and 0.1% Triton X-100 for 20 min, followed by washing with PBS. After blocking with 5% bovine serum albumin for 30 min, the cells were incubated with the primary antibody overnight at 4 °C. The secondary antibodies were applied at room temperature for 2 h, followed by washing with PBS and nuclear staining with DAPI. Glass coverslips carrying the cells were mounted with glycerol and examined under a fluorescence microscope. Primary antibodies against the following targets were used: TH (Santa Cruz Biotechnology, sc-25269, 1:400), TRHR (Novus Biologicals, NBP2-24726, 1:200), GABA (Abcam, ab86186, 1:200), RARα (ABclonal, A0370, 1:200), DRD1 (Novus Biologicals, NB110-60017, 1:200), DRD2 (Novus Biologicals, MAB9266, 1:200), and RARα (ABclonal, A0370, 1:200).

Statistical analysis

All data are presented as the mean ± SEM from three or more independent experiments and plotted using GraphPad Prism (version 9.0). One-way analysis of variance (one-way ANOVA) was applied to determine significant main effects and differences among three or more groups, followed by post hoc tests such as Tukey's or least significant difference (LSD) multiple comparisons. Student's t-test was applied for comparing two groups. Statistical significance was defined as $p < 0.05$. The conditions of the analysis were blinded to the investigator.

Results

TAL-induced alterations in key signaling pathways and cellular components in the striatum

Transcriptomic profiling study with the striatum samples of Hemi-PD Rats treated by TAL highlights the significance of the calcium signaling pathway, MAPK signaling pathway and Axon guidance in influencing GABAergic and DA synapses.

The apomorphine-induced rotation test, adjusting step test, and TH staining were conducted to validate the success of the Hemi-PD rat model. TH-positive dopaminergic terminals in the striatum on the lesioned side were almost destroyed (Fig. 1A). Successful hemi-PD rats were separately administered saline or TAL at a dose of 5 mg/kg via intraperitoneal injection. At 0.5 h post-injection, the TAL-treated (TAL, N = 8) group showed alleviation of bradykinesia symptoms in the forelimbs compared to the control group (CTR, N = 8) (Fig. 1B). To investigate the specific gene expression mechanisms through which TAL exerts its effects in the striatum, we extracted RNA from the intact side of the control group (CTR-Int), the lesioned side of the control group (CTR-Les), the Intact side of the TAL-treated group (TAL-Int) and the lesioned side of the TAL-treated group (TAL-Les) after 7 days of TAL intraperitoneal injection for transcriptomic analysis. Differential gene analysis was performed using DEGSeq, with conditions set as $|\log2FC| \geq 2$ and adjusted P-value < 0.05. Volcano plots were generated to display the DEGs among the groups. Compared to the CTR-Int group, the CTR-Les group exhibited upregulation of 3046 transcripts and downregulation of 4299 transcripts (Fig. 1C). Compared to the CTR-Les group, the TAL-Les group exhibited upregulation of 4352 transcripts and downregulation of 3848 transcripts (Fig. 1D). Compared to the CTR-Int group, the TAL-Int group exhibited upregulation of 3407 transcripts and downregulation of

4242 transcripts (Supplementary Fig. 1A). Compared to the TAL-Int group, the TAL-Les group exhibited upregulation of 3576 transcripts and downregulation of 3535 transcripts (Supplementary Fig. 1B). We observed a decrease in the gene expression of the *trhr* in the lesioned side of hemi-PD rats, which is the target receptor of TAL. Meanwhile, TAL upregulated the expression of *rarα* and cAMP-responsive element binding protein 1 (*creb*) and activated certain genes in the calcium signaling pathway. Quantitative RT–PCR was performed to validate the gene expression levels of *Trhr*, *Rarα*, *Creb* and calcium/calmodulin-dependent protein kinase II beta (*Camk2b*) in the striatum of each group (Fig. 1E), which were consistent with the transcriptomic analysis results. We further verified the protein expression levels of CREB and CaMK2b in the striatum of each group using Western blotting analysis (Fig. 1F). The results were consistent with the mRNA changes, showing significant expression of CREB and CaMK2b in the TAL-Les group.

Furthermore, clustering analysis was conducted using the log2-transformed FPKM values of the DEGs. GO enrichment analysis was performed to explore the anatomical locations of the DEGs in the striatal cells. Significant changes in gene expression were observed in cell components related to neuron projection, neuronal cell bodies, dendrites, and postsynaptic density on the lesioned side (Fig. 1I), while TAL mainly affected GABAergic synapses in the striatal cell components (Fig. 1J). Meanwhile, on the intact side of the striatum, compared to the CTR-Int group, TAL affected cell components such as neuron projections and transcription factor complexes (Supplementary Fig. 1C). On the lesioned side, compared to the TAL-Int group, TAL primarily affected components like nucleoplasm and nucleus (Supplementary Fig. 1D).

To elucidate the cellular functional changes induced by TAL, we performed functional annotation of the DEGs using the EggNOG database. In the Hemi-PD rats, the functional changes on the lesioned side were mainly associated with calcium-dependent phospholipid binding (Fig. 2A), while TAL treatment primarily affected DNA binding and protein serine/threonine kinase activity (Fig. 2B). DNA binding involves the interaction between a molecular entity, exemplified prominently by transcription factors, and the DNA molecule. Serine/threonine kinases utilize ATP as a phosphate donor to catalyze the phosphorylation of serine or threonine residues on target proteins. They encompass protein kinases activated by second messengers such as cAMP, cGMP, Ca^{2+}, and DAG, as well as the MAPK cascade.

To further understand the specific signaling mechanisms underlying the actions of TAL, we performed KEGG pathway classification analysis on the DEGs from each group. In the Hemi-PD rat striatum, the changes in signaling pathways were mainly associated with the calcium signaling pathway, neuroactive ligand–receptor interaction, cAMP signaling pathway, cGMP-PKG signaling pathway, and Wnt signaling pathway (Fig. 2C). After TAL treatment, significant changes were observed in the lesioned side of the striatum, particularly in the calcium signaling pathway, MAPK signaling pathway, axon guidance, cGMP-PKG signaling pathway, and dopaminergic synapse (Fig. 2D). On the intact side of the striatum, compared to the CTR-Int group, TAL affected signaling pathways such as the Calcium signaling pathway and Neuroactive ligand-receptor interaction (Supplementary Fig. 1E). On the lesioned side, compared to the TAL-Int group, TAL primarily influenced signaling pathways like Axon guidance and cGMP-PKG signaling pathway (Supplementary Fig. 1F).

DA synapses consist of presynaptic dopaminergic terminals and postsynaptic GABAergic synapses. In humans, dopaminergic neurons in the midbrain project densely to the striatum and form DA synapses on principal neurons of the striatum, known as MSNs. Based on the interactions among these pathways, we constructed a KEGG network pathway map to illustrate the relationships between transcripts and signaling pathways. The findings unveiled intricate interactions within these signaling pathways (Fig. 2E), wherein TAL influenced the

(See figure on next page.)

Fig. 1 Transcriptomic analysis of the striatal in Hemi-PD Rats following TAL treatment. **A** Immunostaining of TH in the striatum of Hemi-PD rats (Scale bar: 1000 μm, N = 8/group, mean ± SEM). Statistical significance: ****$P < 0.0001$, Student's t-test. **B** Adjusting step tests of Hemi-PD Rats treated with saline or TAL (5 mg/kg, i.p.). N = 8. **C**, **D** Volcano plots of DEGs. Comparison of gene expression changes between the lesioned side of the control group (CTR-Les) and the intact side of the control group (CTR-Int), the lesioned side of the TAL-treated group (TAL-Les) and the CTR-Les group. Blue dots represent downregulated DEGs, and red dots represent upregulated DEGs (*q-value* < 0.05, |log2*FC* |≥ 2). **E** RT-PCR analysis shows the expression levels of *trhr*, *rara*, *creb* and *camk2b* mRNA in the striatum (N = 8/group, mean ± SEM). Statistical significance: **$P < 0.01$, ****$P < 0.0001$, one-way ANOVA followed by Tukey's test. **F** Western blot analysis of CREB and CAMK2B levels in the striatum of different groups of rats (N = 8/group; error bars represent SEM). Statistical significance: *$P < 0.05$, **$P < 0.01$, ****$P < 0.0001$, one-way ANOVA followed by Tukey's test. **I**, **J** Gene Ontology (GO) enrichment analysis of transcripts. The X-axis represents the enrichment ratio, the Y-axis represents the GO cellular component term, and the size of the bubbles indicates the number of DEGs annotated to a particular term. The color represents the *P*-value of enrichment, with a smaller *P*-value indicated by a redder color

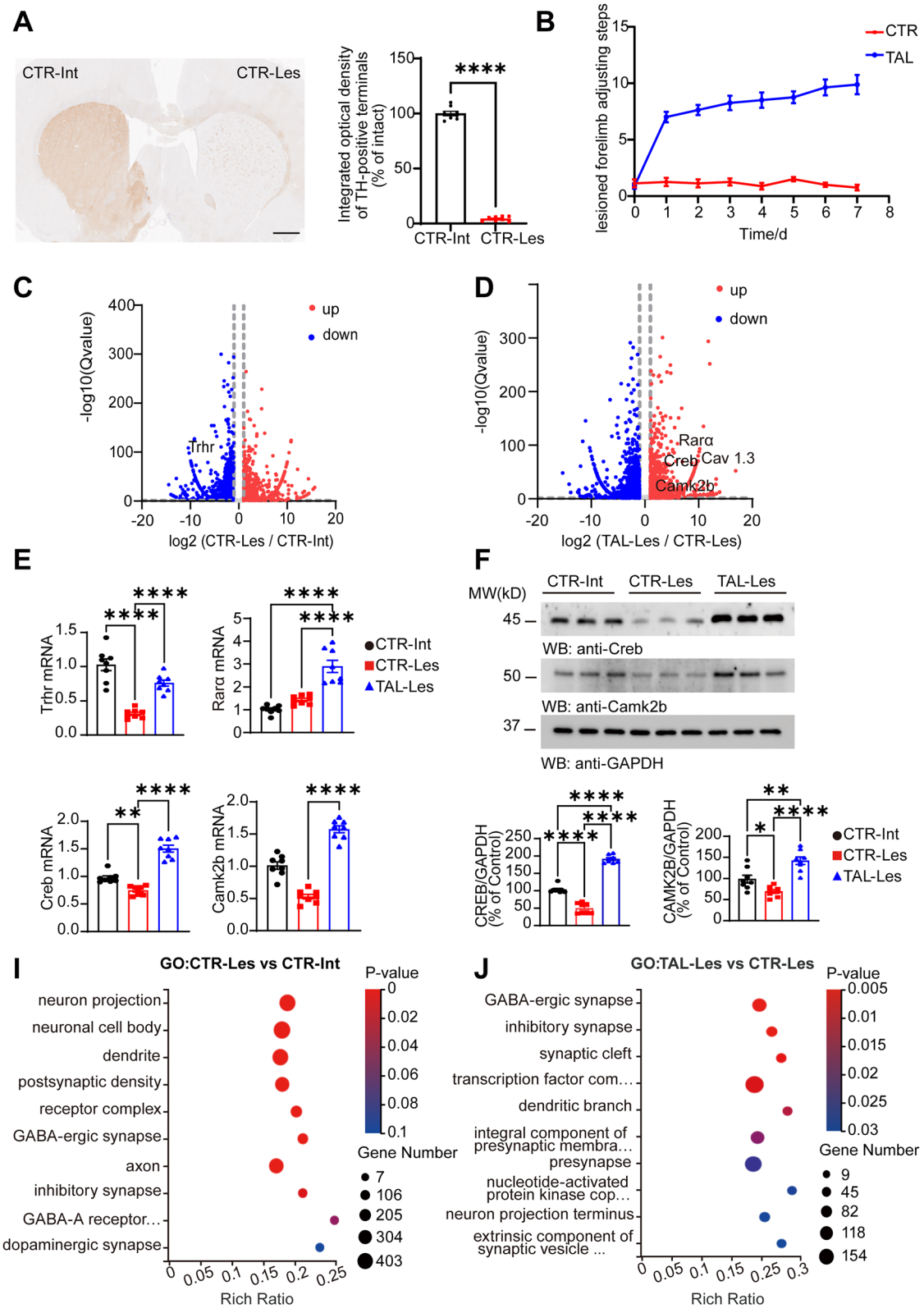

Fig. 1 (See legend on previous page.)

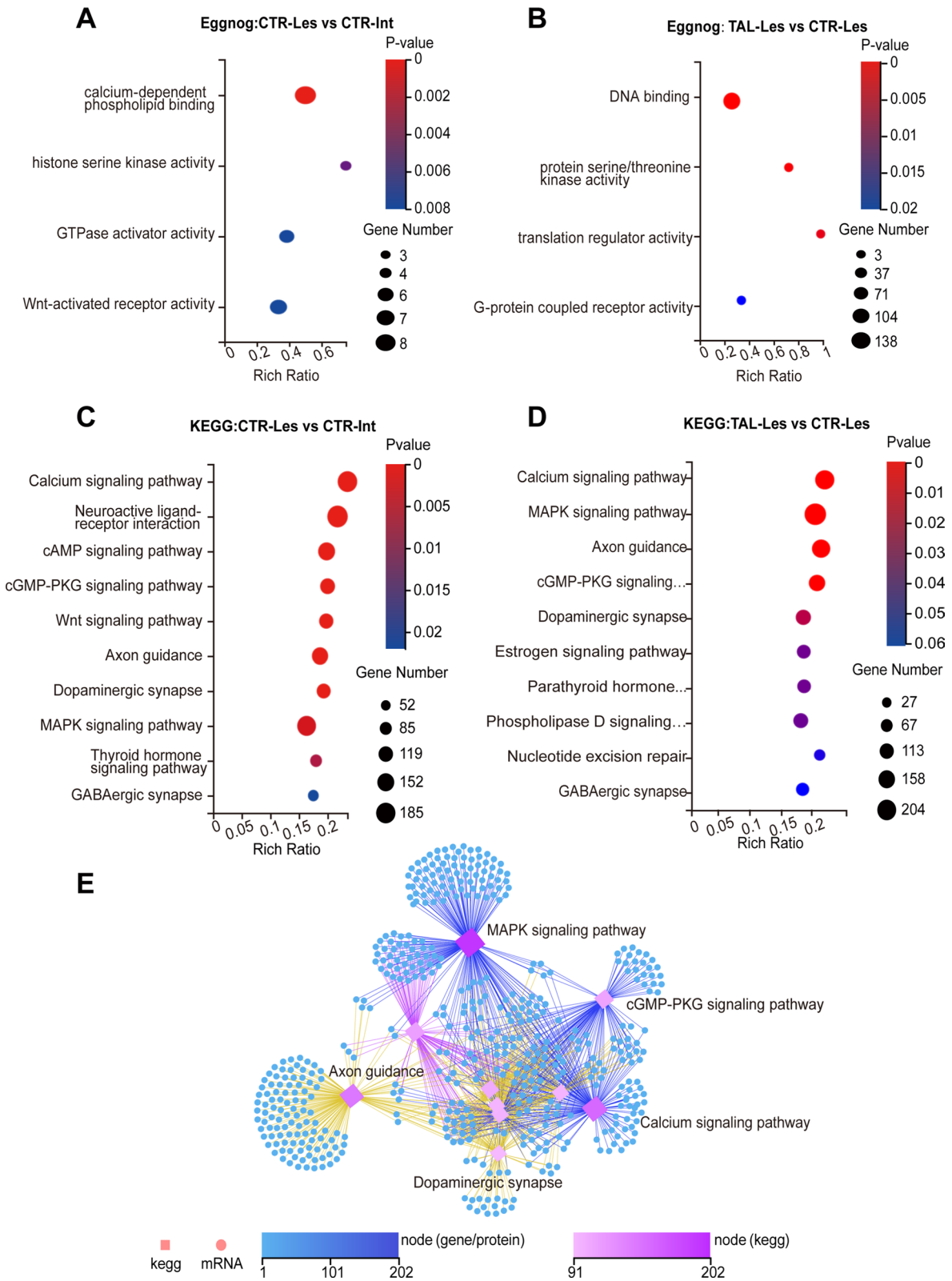

Fig. 2 TAL modulates intracellular signaling pathways. **A**, **B** Functional annotation of the striatal transcriptome using Eggnog. **C**, **D** KEGG enrichment analysis of transcripts. DEGs are divided into 10 KEGG pathway terms along the y-axis. **E** Ranking of KEGG pathways based on the number of genes associated with selected genes. The top 10 pathways with the highest gene count are displayed. Squares represent KEGG pathways, circles represent mRNAs, and the color and size indicate the number of transcripts connected to each node

MAPK signaling pathway. This, in turn, triggers modifications in axon guidance, the cGMP-PKG signaling pathway, and the calcium signaling pathway. Consequently, a cascading sequence of events led to alterations in the DA synapses within the striatum.

By integrating the differentially expressed transcripts into the classical DA synaptic pathway diagram, the impact of TAL on gene expression becomes evident. Notably, TAL influences the expression of genes such as *th*, *drd2,* and *vmat* in the presynaptic pathway. Furthermore, it induces altered gene expression of key signals encompassing DRD2, Gi/o, PLC, PKA, PKC, CREB, and MAPK in the postsynaptic pathway (Fig. 3A). Within the dopaminergic synapse, a total of 23 shared genes exhibited a decrease in expression in the CTR-Les vs. CTR-Int comparison and an increase in the TAL-Les vs. CTR-Les comparison (Fig. 3B). The expression levels of these 23 shared genes in the CTR-Int, CTR-Les, and TAL-Les groups were visualized through a clustering heatmap (Fig. 3C).

Within the calcium signaling pathway, TAL not only influences the expression of key components, including TRHR and other G protein-coupled receptors (GPCRs) but also triggers two distinct pathway modifications: one involving GPCR-Gq-PLC-IP3R and the other implicating GPCR-Gs-ADCY-PKA. Additionally, TAL directly impacts voltage-gated calcium channels (Supplementary Fig. 2A). Within the calcium signaling pathway, a collective total of 26 genes shared among the studied groups exhibited reduced expression in the CTR-Les vs. CTR-Int comparison but augmented expression in the TAL-Les vs. CTR-Les comparison (Supplementary Fig. 2B). These expression patterns of the 26 shared genes within the CTR-Int, CTR-Les, and TAL-Les groups are effectively depicted through a clustering heatmap (Supplementary Fig. 2C). Furthermore, in the cGMP-PKG signaling pathway, certain genes in the GPCR-PLC-IP3R signaling pathway were also observed to be affected by TAL (Supplementary Fig. 3A, C). Within the context of the cGMP-PKG signaling pathway, a total of 16 shared genes exhibited decreased expression in the CTR-Les vs. CTR-Int comparison, while revealing increased expression in the TAL-Les vs. CTR-Les comparison (Supplementary Fig. 3B). The expression profiles of these 16 shared genes within the CTR-Int, CTR-Les, and TAL-Les groups are effectively illustrated through a clustering heatmap (Supplementary Fig. 3C).

In the MAPK signaling pathway, TAL influences three cascades, namely, the classical MAP kinase pathway, the JNK and p38 MAP kinase pathway, and the ERK5 pathway (Supplementary Fig. 4A). Within the MAPK signaling pathway, a total of 28 shared genes exhibited diminished expression in the CTR-Les vs. CTR-Int comparison while manifesting enhanced expression in the TAL-Les vs. CTR-Les comparison (Supplementary Fig. 4B). The expression profiles of these 28 shared genes among the CTR-Int, CTR-Les, and TAL-Les groups are aptly illustrated through a clustering heatmap (Supplementary Fig. 4C).

In the axon guidance pathway, TAL elevates the gene expression levels of the Netrin family, including Netrin-1 and Netrin-G1, and influences the subsequent expression of NGL-1 and DCC receptors, thereby guiding axon growth (Supplementary Fig. 5A). Within the axon guidance, a collective set of 24 genes exhibited reduced expression in the CTR-Les vs. CTR-Int comparison but showed heightened expression in the TAL-Les vs. CTR-Les comparison (Supplementary Fig. 5B). A clustering heatmap (Supplementary Fig. 5C) effectively portrays the expression patterns of these 24 shared genes across the CTR-Int, CTR-Les, and TAL-Les groups.

Apart from the aforementioned principal signaling pathways, TAL also exerts its influence on the estrogen signaling pathway (Fig. 2D). We observed that within the estrogen signaling pathway, accompanied by changes in PKA and PKC, the transcription factors pCREB and RARα were activated (Supplementary Fig. 6A). Within the estrogen signaling pathway, a collective assemblage of 14 genes exhibited diminished expression in the CTR-Les vs. CTR-Int comparison, while concurrently manifesting amplified expression in the TAL-Les vs. CTR-Les comparison (Supplementary Fig. 6B). These expression profiles of the 14 shared genes across the CTR-Int, CTR-Les, and TAL-Les groups were effectively visualized through a clustering heatmap (Supplementary Fig. 6C).

TAL modulates TRHR and TH in MSNs

We observed intriguing changes in TRHR, the binding site of TAL in the striatum (Figs. 1C, 2B, Supplementary Fig. 2C). To further explore these specific changes, we performed Western blotting and immunohistochemistry. The results demonstrated that the expression levels of TRHR and TH were significantly lower on the lesioned side of the Hemi-PD rat striatum than in the control group, whereas TAL markedly increased the expression of TRHR and TH within the lesioned side of the striatum (Fig. 4A, B, C). Immunohistochemical analysis of the striatum also confirmed that TAL elevated the number of positive neurons expressing TRHR (Fig. 4D, E).

The synergistic expression of TRHR and TH in the striatum of the PD model intrigued us and raised the question of a potential relationship between them. The immunofluorescence results not only confirmed that TAL regulated the expression of TRHR and TH on dopaminergic neuron axons but also revealed the presence of a certain level of TRHR and TH expression outside the

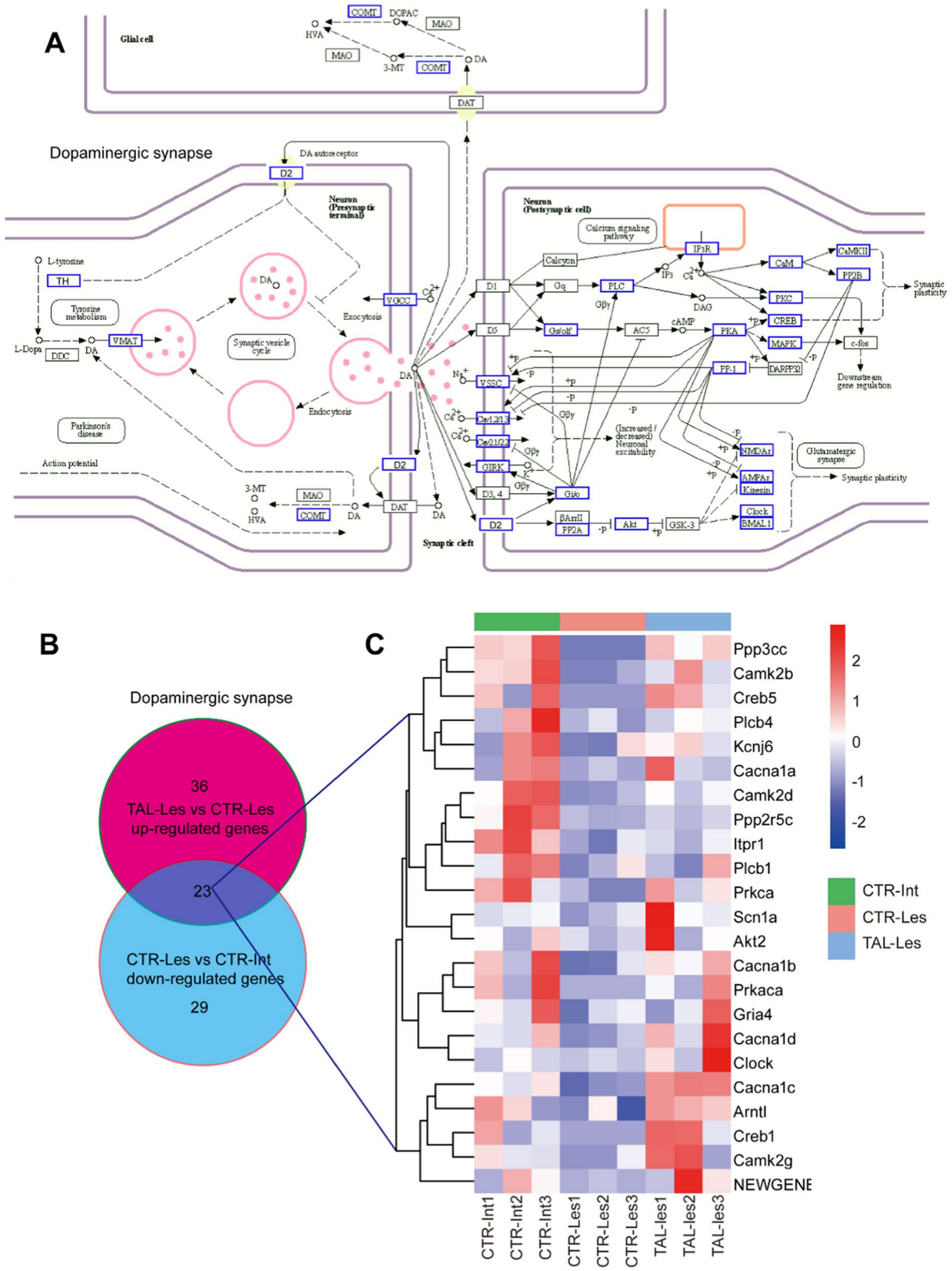

Fig. 3 TAL modulates the dopaminergic synapse signaling pathway. **A** KEGG Pathway Map (04728). In the classical dopaminergic synapse signaling pathway, the differential signals induced by TAL are highlighted in blue. **B** The number of common genes in opposite trends between TAL-Les vs. CTR-Les and CTR-Les vs. CTR-Int (*q-value* < 0.05, |log2*FC*| ≥ 2). **C** The shared genes resulting from the comparison depicted in (B). In the heatmap, the red and blue colors correspond to high-expression and low expression levels, respectively

axons on the lesioned side of the striatum, with clear colocalization in neurons (Fig. 4F).

To validate the neuronal type in which the expression levels were altered, we performed immunofluorescence double-labeling of TRHR with GABA, DRD1, and DRD2 proteins in the lesioned side of the striatum in the TAL treatment group. The results indicated that increased TRHR was present on GABAergic neurons and mainly colocalized with DRD2 (Fig. 5A). The colocalization coefficient of TRHR with GABA was 0.75, that with DRD1 was 0.40, and that with DRD2 was 0.88 (Fig. 5B, C, D). We also performed immunofluorescence colocalization studies of TH with GABA, DRD1, and DRD2 in the lesioned side of the striatum in the TAL treatment group (Supplementary Fig. 7A). Additionally, we conducted co-staining of TH with the MSNs marker CTIP2 and the microglial marker IBA1 in the lesioned side of the striatum (Supplementary Fig. 7A). The results confirm that TAL primarily affects the expression of TH in MSNS.

TAL induces increased expression of RARα and DRD2 by activating ERK/p-ERK.

In addition to enhancing the expression of TRHR and TH, we observed an elevation in DRD2 expression on the lesioned side of the striatum in the TAL treatment group, as revealed by immunofluorescence results (Figs. 6A, C, 7A). DRD2 plays a crucial role in the treatment of PD, and changes in its expression are of great significance to the nervous system. Furthermore, immunofluorescence reveals that dopaminergic neurons in the substantia nigra express DRD2 (Supplementary Fig. 7B). RARα, a nuclear receptor that forms heterodimers with its target response elements, regulates gene expression in various biological processes and has been shown to modulate DRD2 expression [37]. Our omics findings also underscore the significant transcriptional role played by RARα in the mechanism of action of TAL (Supplementary Fig. 6A). Immunofluorescence confirmed that TAL increased the expression levels of RARα in the TAL-les group striatum (Fig. 6B, D). Furthermore, fluorescence colocalization revealed that after 7 days of TAL treatment, both RARα and DRD2 were coexpressed in neurons on the lesioned side of the striatum in the PD model (Fig. 6E). Based on the results of omics analysis, we hypothesized that the MAPK pathway played a crucial role in this signaling cascade, and extracellular signal-regulated kinase (ERK), as a classical protein in the MAPK pathway, could phosphorylate various transcription factors and enhance their expression.

We validated the expression levels of phosphorylated ERK1/2 (p-ERK1/2) in the striatum of different groups of rats using Western blotting. The results demonstrated that TAL significantly activated the expression of p-ERK1/2 (Fig. 6F, G), which subsequently led to increased expression levels of RARα and DRD2 on the lesioned side of the striatum (Fig. 6F, H, I).

We also confirmed these findings in SH-SY5Y cells. SH-SY5Y, a human neuroblastoma cell line, serves as a mature and widely used in vitro model for PD [38]. TAL at a concentration of 5 μM showed the highest proliferation rate for SH-SY5Y cells [20]. After treating the cells with 5 μM TAL for 48 h, we examined the distribution and expression of TRHR, DRD2, and RARα in the cells using immunofluorescence. Compared to the control group treated with physiological saline, TAL significantly increased the fluorescence intensity of TRHR, RARα, and DRD2 (Fig. 7A, B, C, D). Additionally, we observed a marked increase in the coexpression of TRHR with DRD2 and DRD2 with RARα after TAL treatment (Fig. 7E, F).

To validate these findings, Western blotting was performed on the control and TAL-treated SH-SY5Y cell groups. The results confirmed that TAL increased the protein expression levels of p-ERK1/2, TRHR, RARα, and DRD2 in the cells (Fig. 7G, H).

Subsequently, we employed Flag-His-TRHR plasmids and siRNA-TRHR transfection in SH-SY5Y cells to manipulate the expression levels of TRHR. After 48 h, we confirmed the downregulation and upregulation of TRHR expression in the cells, followed by a 24-h incubation with TAL (5 μM) to assess the protein expression levels in each group. The results revealed that overexpression of TRHR (OE group) led to an increase in TRHR expression, accompanied by upregulation of p-ERK, RARα, and DRD2 expression. Even in the case of TRHR knockdown, TAL still increased TRHR expression and activated p-ERK1/2, resulting in increased expression levels of RARα and DRD2. This suggests that TAL can exert its effects with only a small amount of TRHR

(See figure on next page.)

Fig. 4 TAL regulates the expression of both TRHR and TH in the striatum. **A, B, C** Western blot analysis of TRHR and TH levels in the striatum of different groups of rats.Differential analysis of TRHR **B** and TH **C** in the striatum of different groups (N = 8/group; error bars represent SEM). Statistical significance: ****$P < 0.0001$, one-way ANOVA followed by Tukey's test. **D** Immunohistochemical images of TRHR in the striatum of different groups of rats (CTR-Int, CTR-Les, TAL-Les). Scale bar: 200 μm. **E** Differential analysis of TRHR-positive cell counts in the striatum of different groups (N = 8/group; error bars represent SEM). Statistical significance: ****$P < 0.0001$, one-way ANOVA followed by Tukey's test. **F** Immunofluorescence staining and colocalization of TH and TRHR in the striatum of various animal groups. Scale bar: 20 μm

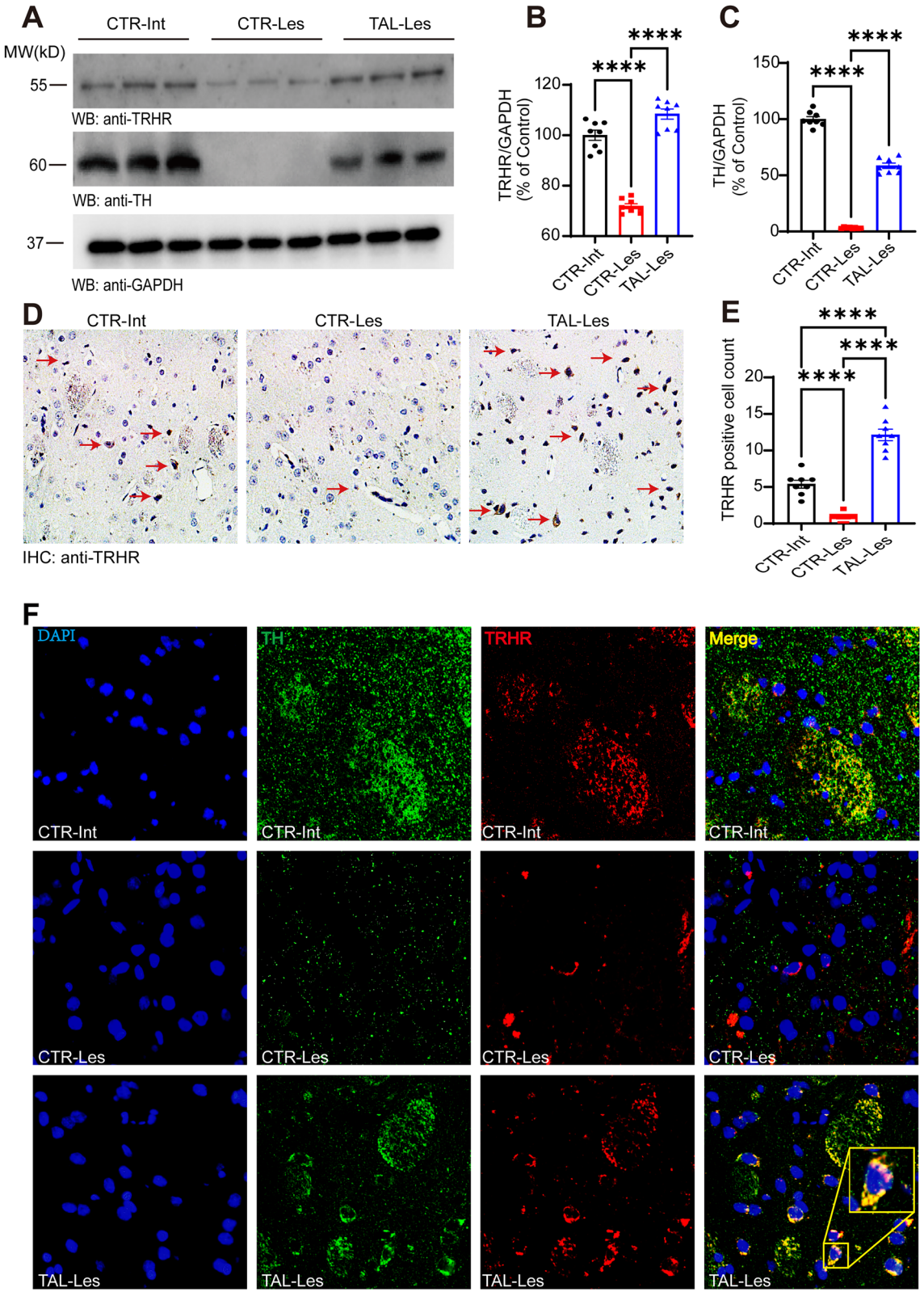

Fig. 4 (See legend on previous page.)

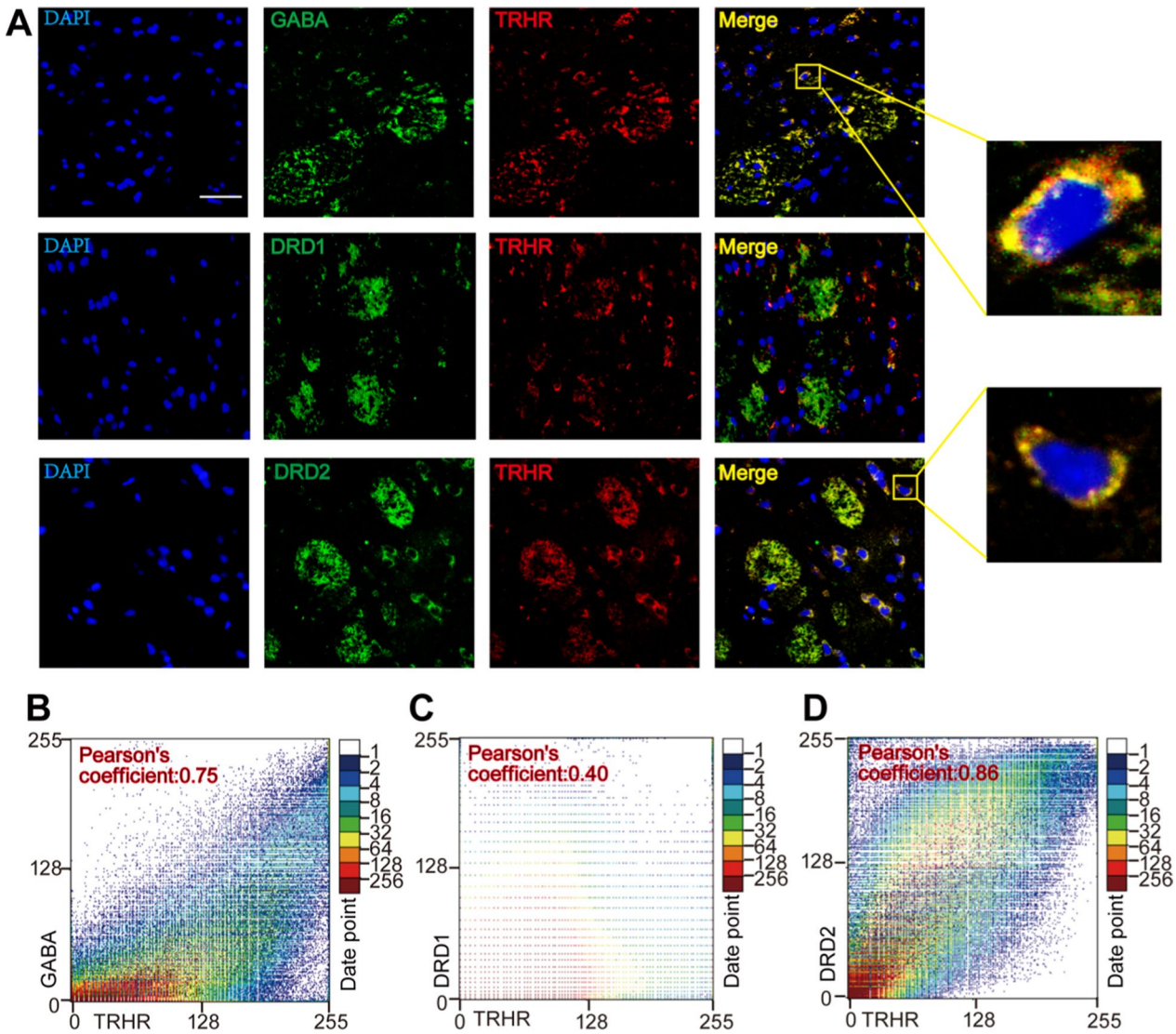

Fig. 5 TRHR and TH mainly colocalize GABAergic neurons. **A** Immunofluorescence colocalization of TRHR with DRD1 and DRD2 in the Lesioned striatum of TAL-treated Hemi-PD rats. Scale bar: 20 μm. **B, C, D** Scatter plots and Pearson correlation coefficients of colocalization

(See figure on next page.)

Fig. 6 TAL enhances the expression of RARα and DRD2 in the striatum. **A**, **B** Immunofluorescence staining of TRHR and RARα in the striatum of different groups of rats (CTR-Int, CTR-Les, TAL-Les). Scale bar: 25 μm. **C**, **D** Analysis of relative fluorescence intensity (N = 8/group; error bars represent SEM). Statistical significance: ****$P < 0.0001$, one-way ANOVA followed by Tukey's test. **E** Immunofluorescence colocalization of DRD2 and RARα in the striatum. **F** Western blotting analysis of P-ERK1/2, ERK1/2, RARα, and DRD2 levels in the striatum of different groups of rats. **G, H, I** Differential analysis of P-ERK1/2, RARα, and DRD2 in the striatum of different groups (N = 8/group; error bars represent SEM). Statistical significance: ****$P < 0.0001$, one-way ANOVA followed by Tukey's test

present. Among the cell groups, OE + TAL exhibited the most significant elevation in the expression levels of TRHR, p-ERK1/2, RARα, and DRD2 (Fig. 7I, J).

Therefore, both in vitro and in vivo experiments demonstrate that TAL enhances the expression of TRHR, subsequently activating the MAPK signaling pathway, leading to increased expression of the transcription factor RARα and resulting in elevated DRD2 expression (Fig. 8).

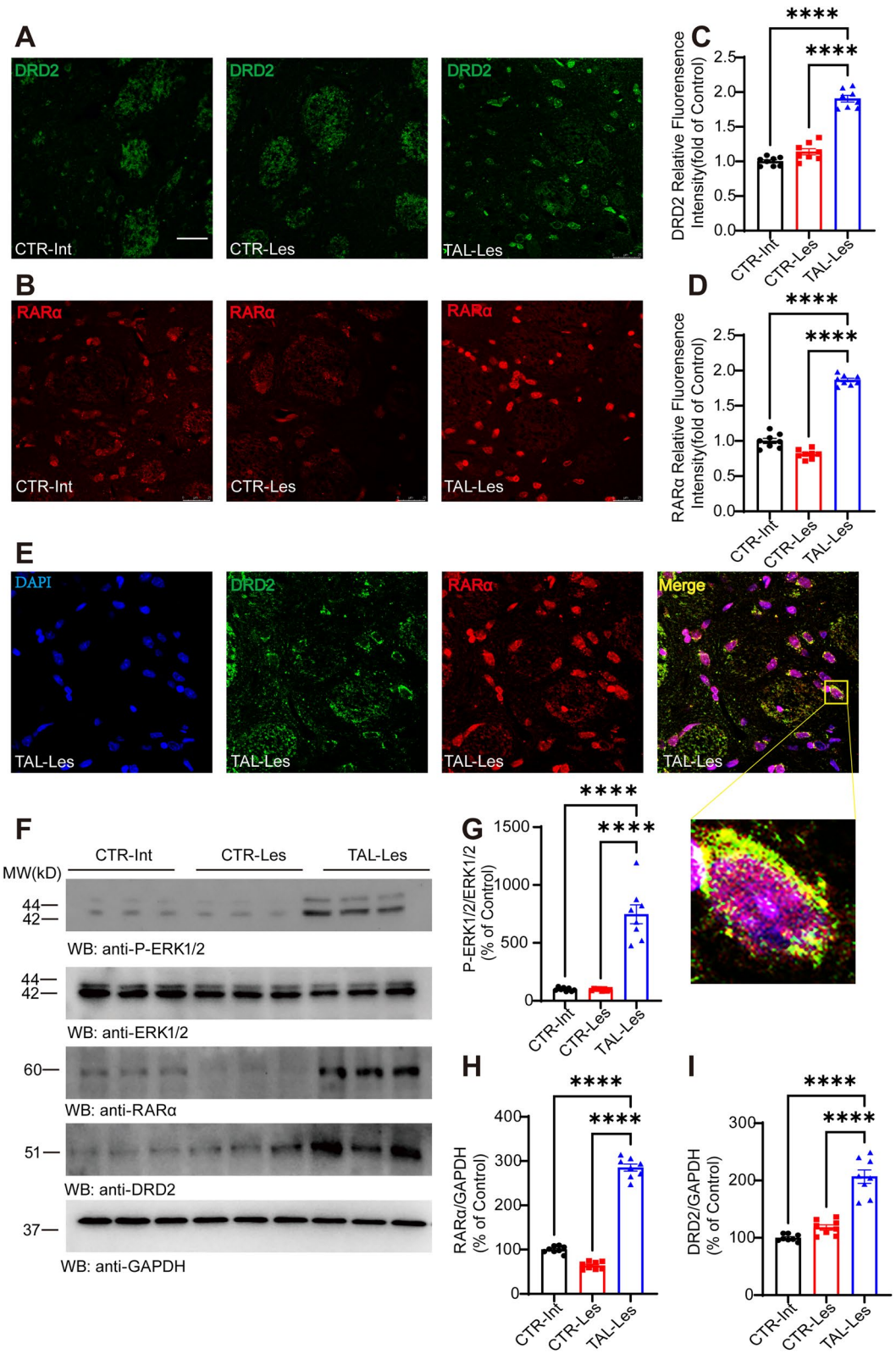

Fig. 6 (See legend on previous page.)

Discussion

As an effective TRH analog, TAL has been shown to possess neuroprotective effects in cellular and animal models of PD, and it can promote central nervous system release of DA in a mild and sustained manner, thereby improving motor function without less fluctuation [7, 20, 21, 39, 40]. However, the specific molecular mechanisms underlying its action in the striatum remain unclear, limiting its clinical application for the treatment of PD. In this study, a variety of in vivo and in vitro methods, including transcriptomic analysis, were conducted to elucidate the application of TAL in hemi-PD rats, demonstrating that TAL increases the expression levels of TRHR on D2-MSNs and activates multiple pathways, including the MAPK pathway, to regulate the expression of RARα, DRD2, and TH.

TRHR is a GPCR primarily expressed in cells involved in thyroid hormone secretion [41]. In rodents, TRHR has two subtypes. In contrast, humans have a single type of TRHR that is more similar to TRHR1 in rodents [42]. TRHR not only plays a crucial role in the TRH axis but also plays a significant role in neurological disorders, including antidepressant effects, antiepileptic effects, cognitive enhancement, and improvement of motor symptoms [43]. However, the specific mechanisms underlying its effects are not yet clear. In this experiment, we observed a downregulation of TRHR expression in the striatum of hemi-PD rats, while TAL treatment significantly neutralized this reduction. This differs from the general signaling pathway system composed of receptors and ligands, which are generally balanced by negative feedback regulation. This unusual positive feedback modulation makes the drug less susceptible to intolerability, which is a significant advantage over L-DOPA, the classic medicine for PD. Importantly, although TAL has minimal impact on the endocrine axis, the increased expression of TRHR in the striatum suggests that preassessment and periodic testing of thyroid function in patients is crucial during clinical administration.

In addition, the transcriptomic data reveal that TAL exerts its effect through the calcium signaling pathway, MAPK signaling pathway, axon guidance and cGMP-PKG signaling pathway in influencing DA synapses. Meanwhile, TAL upregulated the expression of *rarα* and *creb*. CREB, as a transcription factor regulating various growth processes, has been shown to activate TRHR expression. Therefore, we propose that TAL, upon activating TRHR in MSNs and subsequently activating the MAPK-ERK1/2 signaling pathway and other signaling pathways, results in increased expression of the transcription factor CREB and, consequently, elevated TRHR expression.

Our previous research has demonstrated that TAL can increase TH expression levels both in vivo and in vitro [21]. In this study, while verifying this effect in a PD animal model, we unexpectedly discovered that TAL can also upregulate the expression of DRD2, enhancing the response to dopaminergic stimulation and alleviating motor impairments. Furthermore, DRD2 expression was closely related to the MAPK-RARα pathway [44]. We also confirmed that TAL increased the activation of p-ERK and the expression of RARα. Through immunofluorescence, we found that newly appearing TH-positive neurons in the striatum after TAL treatment exhibited significant colocalization with increased TRHR and DRD2 expression. The results of this experiment suggest that the TH-positive neurons induced by TAL are closely associated with DRD2 rather than DRD1.

However, studies have shown that in PD models, the number of TH-positive neurons in the striatum increases after treatment with L-DOPA [45] and may be associated with DRD1 [8]. Additionally, a subset of GABAergic interneurons in the striatum can also express TH (THINs) and has been demonstrated to be upregulated in PD models [8, 9, 29]. However, these TH-expressing interneurons do not metabolize dopamine; instead, they utilize TH through different pathways, preventing them from being classified as dopaminergic [28, 29]. CTIP2 is one of the well-recognized markers of striatal MSNs and has been shown to be absent in interneurons [46]. Although we demonstrated through colocalization of TH and CTIP2 that the increased expression of TH-positive neurons is primarily located in MSNs, the possibility that TAL induces a transformation of D1-MSNs, leading to increased expression of both TH and DRD2, cannot

(See figure on next page.)

Fig. 7 TAL enhances the expression of TRHR and DRD2 in SH-SY5Y cells. **A**, **B** Immunofluorescence colocalization of DRD2 with TRHR and RARα in SH-SHY5Y cells of the CTR and TAL groups. Scale bar: 25 μm. **C**, **D** Analysis of the relative fluorescence density of DRD2 and RARα in cells from the CTR and TAL groups (N = 8/group; error bars represent SEM). Statistical significance: ****$P < 0.0001$, Student's t-test. **E**, **F** Analysis of the count of colocalized positive cells of DRD2 with TRHR and RARα in different groups of cells (N = 8/group; error bars represent SEM). Statistical significance: ****$P < 0.0001$, Student's t-testt. **G**, **H** Western blotting analysis of TRHR, P-ERK1/2, ERK1/2, RARα, and DRD2 levels in the SH-SY5Y of CTR and TAL group (N = 8/group; error bars represent SEM). Statistical significance: ****$P < 0.0001$, Student's t-test. **I**, **J** After knockdown and overexpression of TRHR, Western blotting analysis of TRHR, P-ERK1/2, ERK1/2, RARα, and DRD2 levels in each group of SH-SY5Y cells (N = 8/group; error bars represent SEM). Statistical significance: **$P < 0.01$, ****$P < 0.0001$, one-way ANOVA followed by Tukey's test

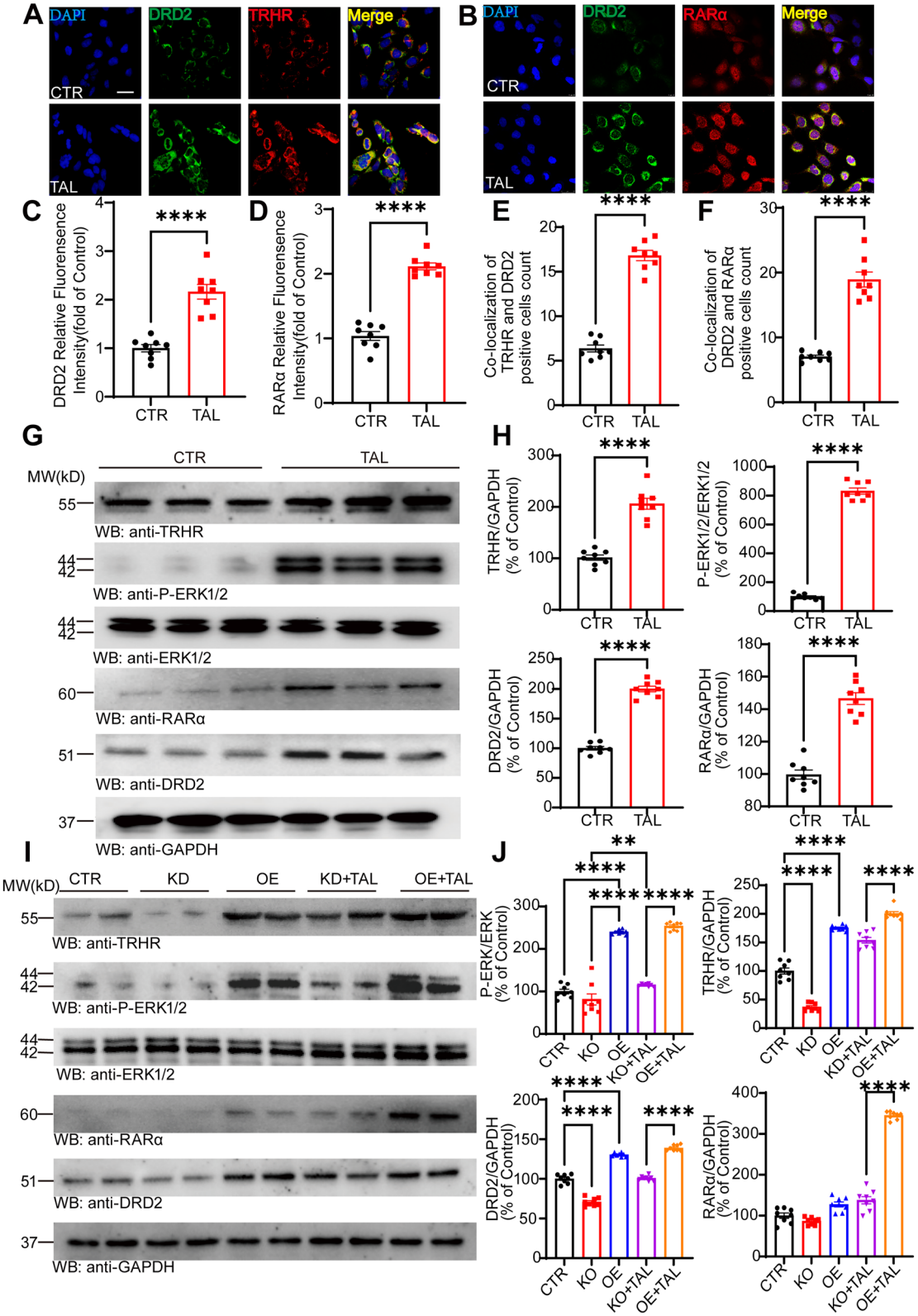

Fig. 7 (See legend on previous page.)

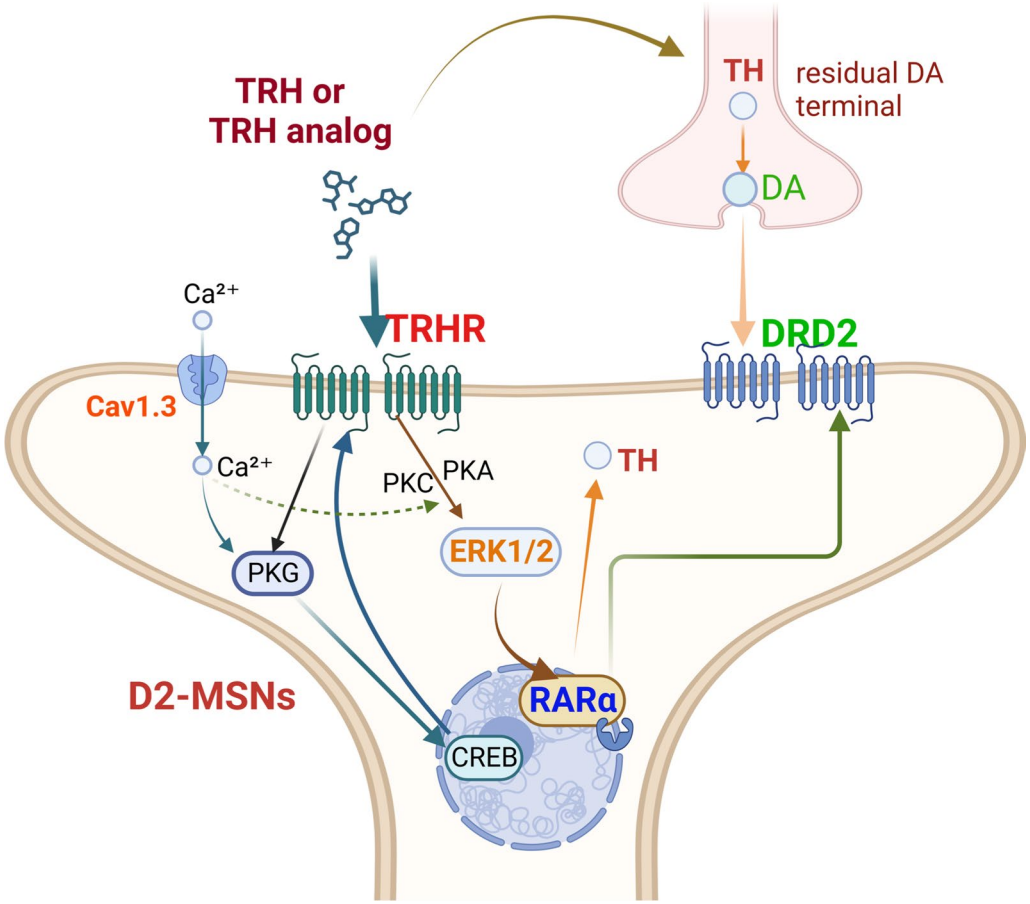

Fig. 8 The mechanism of TAL in PD models. Our results demonstrated that TAL administration in hemi-PD rats led to increased expression of TH in the remaining dopaminergic axonal terminals within the striatum. Furthermore, TAL binds to TRHR, which is primarily expressed on GABAergic neurons such as D2-MSNs. Upon TRHR activation, various potential signaling pathways are initiated, leading to increased CREB and p-ERK1/2 activity. This activation further promotes the upregulation of TRHR and RARα expression. RARα, in turn, regulates DRD2 expression. As a result, TAL induces MSNs to express TH

be ruled out. Whether TAL induces changes in other dopamine-synthesizing enzymes within these neurons also requires further investigation. Further research is needed to explore this possibility in the future.

DRD2 plays a crucial role in the treatment of PD and various movement disorders. Commonly used DA receptor agonists, such as pramipexole, primarily target DRD2 receptors. TAL may assist DA receptor agonists in achieving more efficient therapeutic effects. Motor complications during the treatment of PD, especially L-DOPA-induced dyskinesia, are thought to be closely related to DRD1 receptors [47–51]. The positive regulation of DRD2 receptors by TAL suggests that the drug can better avoid motor complications, which is another major advantage over L-DOPA. However, it is important to note that DRD2 is also a target of many antipsychotic drugs used to suppress positive symptoms by antagonizing DRD2, exerting a neuroleptic effect [52]. Therefore, caution should be exercised when using TAL in patients with psychiatric symptoms.

In this study, we found that the expression of RARα is regulated by TAL. The ability of retinoic acid (RA) to induce cell differentiation has been used in cancer treatment [53, 54] and guided embryonic stem cell differentiation in regenerative medicine [55]. In humans and animals, retinol is first converted to retinaldehyde and then converted to RA in cells that can utilize retinaldehyde, such as dopaminergic neurons expressing TH in their axons and terminals [56]. RARα regulates transcription in a ligand-dependent manner and is associated with development, differentiation, and apoptosis, playing a significant role in brain function [57]. RA not only regulates DRD2 expression [37] but also plays a critical role in the differentiation of functional DA neurons [58]. RA induces the generation of MSNs in the striatum from pluripotent stem cells, and RARα

promotes the differentiation of pluripotent stem cells into a subgroup of DA-producing neurons expressing TH, which also exhibit GABAergic properties [59]. In our experiment, TAL significantly increased RARα expression on the lesioned side of striatum in the PD model and elevated RARα expression in SH-SY5Y cells. Additionally, our transcriptomic data suggest that TAL may influence the estrogen signaling pathways, potentially altering the expression of RARα. However, further studies are needed to validate this finding.

Interestingly, the extent of RARα upregulation correlated not only with TRHR-MAPK pathway activation but also with the TRHR expression level, as RARα increased following the upregulation of TRHR. Transfection of TRHR plasmids into SH-SY5Y cells demonstrated that once TRHR reached a certain level, a small amount of TRH secreted by the cells could activate downstream pathways, indicating the critical role of elevated TRHR levels in the initiation of the effects of TAL.

Considering the aforementioned experimental results, we observed that TAL stimulated an increase in TRHR expression in MSNs. Subsequently, TRHR caused alterations in the MAPK signaling pathway, leading to increased RARα expression. RARα, in turn, upregulated DRD2 expression. This finding is exciting; however, further details require exploration.

Furthermore, our omics analysis has unveiled a noteworthy impact of TAL on the axon guidance pathway, notably highlighted by the upregulation of pivotal genes such as Netrin-1. This discovery not only sheds new light but also paves an innovative avenue for delving into the intricate mechanistic underpinnings of the therapeutic efficacy of TAL against PD. Notably, Netrin-1, a secreted trophic factor belonging to the laminin-related protein family, has gained increasing prominence in the context of PD pathology. During the developmental phase of the midbrain, Netrin-1 assumes a crucial role in guiding GABAergic neurons toward the ventral substantia nigra, effectively constraining the localization of mDA neurons within the dorsal nigral domain [60]. Additionally, Netrin-1 is essential for the maintenance and protection of adult dopaminergic neurons [61]. In postmortem brain samples of PD patients, a significant reduction in Netrin-1 expression was observed compared to that in healthy controls [62]. Silencing Netrin-1 in the midbrain of adult mice induces DCC fragmentation and considerable loss of dopaminergic neurons, resulting in motor deficits. In contrast, overexpression or intracranial administration of recombinant Netrin-1 exhibits neuroprotective and neurorestorative effects in mouse and rat PD models [63]. Moreover, the pivotal role of the axon guidance pathway in axonal growth and synapse formation suggests its potentially crucial involvement in TAL-induced stem cell-like differentiation processes.

In conclusion, the therapeutic effects of TAL in PD rats depend on multiple regulatory mechanisms and the involvement of various signaling pathways. On the one hand, it stimulates the synthesis and release of a small amount of TH in residual dopaminergic terminals. More importantly, TAL upregulates the expression of TRHR and DRD2 on MSNs, which leads to the activation of the TRHR-MAPK-RARα-DRD2 pathway and induces MSNs to express TH. These findings provide additional insights into the application of TAL in neurological disorders and offer new directions for drug development.

Supplementary Information

The online version contains supplementary material available at https://doi.org/10.1186/s12967-024-06020-x.

Additional file 1: Fig. 1. TAL modulates signal pathways in the intact striatum.Volcano plots of DEGs. Comparison of gene expression changes between the TAL-Int group and the CTR-Int group, the TAL-Les group and the TAL-Int group. Blue dots represent downregulated DEGs, and red dots represent upregulated DEGs.Gene Ontologyenrichment analysis of transcripts. The color represents the *P*-value of enrichment, with a smaller *P*-value indicated by a redder color.KEGG enrichment analysis of transcripts. DEGs are divided into 10 KEGG pathway terms along the y-axis. Fig. 2. TAL regulates the calcium signaling pathway.KEGG Pathway Map. In the classical calcium signaling pathway, the differential signals induced by TAL are highlighted in red.The number of common genes with opposite trends between TAL-Les vs. CTR-Les and CTR-Les vs. CTR-Int.The shared genes resulting from the comparison depicted in. In the heatmap, the red and blue colors correspond to high and low expression levels, respectively. Fig. 3. TAL regulates the cGMP-PKG signaling pathway.KEGG Pathway Map. In the classical cGMP-PKG signaling pathway, the differential signals induced by TAL are highlighted in red.The number of common genes with opposite trends between TAL-Les vs. CTR-Les and CTR-Les vs. CTR-Int.The shared genes resulting from the comparison depicted in. In the heatmap, the red and blue colors correspond to high and low expression levels, respectively. Fig. 4. TAL regulates the MAPK signaling pathway. KEGG pathway map. In the classical MAPK signaling pathway, the differential signals induced by TAL are highlighted in red.The number of common genes with opposite trends between TAL-Les vs. CTR-Les and CTR-Les vs. CTR-Int.The shared genes resulting from the comparison depicted in. In the heatmap, the red and blue colors correspond to high and low expression levels, respectively. Fig 5. TAL regulates the axon guidance pathway. KEGG pathway map. In the classical axon guidance pathway, the differential signals induced by TAL are highlighted in red.The number of common genes with opposite trends between TAL-Les vs. CTR-Les and CTR-Les vs. CTR-Int.The shared genes resulting from the comparison depicted in. In the heatmap, the red and blue colors correspond to high and low expression levels, respectively. Fig 6. TAL regulates the estrogen signaling pathway.KEGG pathway map. In the classical estrogen signaling pathway, the differential signals induced by TAL are highlighted in red.The number of common genes with opposite trends between TAL-Les vs. CTR-Les and CTR-Les vs. CTR-Int .The shared genes resulting from the comparison depicted in. In the heatmap, the red and blue colors correspond to high and low expression levels, respectively. Fig 7. TH mainly colocalizes with MSNs. Immunofluorescence colocalization of TH with GABA, DRD1, DRD2, CTIP2 and IBA1 in the lesioned striatum of TAL-treated Hemi-PD rats. Scale bar: 20 μm. Immunoreactivity of two different DRD2 antibodies in the

substantia nigra on both the intact and lesioned sides. Scale bar: 1000 μm.
Table 1. The primer sequences in the experiment.

Acknowledgements
This work was supported by grants from National Natural Science Foundation of China (The Youth Science Fund Project, 81901292) and National Key Research and Development Program of China(2021YFC2502100)to G.C., National Natural Science Foundation of China (81671051,82071183) to Z.Z.

Author contributions
G.C. conceived the project, designed the experiments, analyzed the data, and wrote the manuscript. K.Z., L.M., J.L.,T.W. and L.D. designed and performed most of the experiments. Z.W. provided assistance with the stereotaxic instrument for animal experiments. X.C. and Z.Z. assisted with data analysis and interpretation and critically read the manuscript.

Funding
National Natural Science Foundation of China, 81901292, Guiqin Chen, 82071183, Zhaohui Zhang, Key Technologies Research and Development Program, 2021YFC2502100, Guiqin Chen

Declarations

Competing interests
The authors declare no competing financial interests.

Received: 16 July 2024 Accepted: 20 December 2024
Published online: 30 December 2024

References

1. Daimon CM, Chirdon P, Maudsley S, Martin B. The role of thyrotropin releasing hormone in aging and neurodegenerative diseases. Am J Alzheimers Dis. 2013. https://doi.org/10.7726/ajad.2013.1003.
2. Shimizu T, Tsutsumi R, Shimizu K, Tominaga N, Nagai M, Ugawa Y, et al. Differential effects of thyrotropin releasing hormone (TRH) on motor execution and motor adaptation process in patients with spinocerebellar degeneration. J Neurol Sci. 2020;415: 116927.
3. Kelly JA, Boyle NT, Cole N, Slator GR, Colivicchi MA, Stefanini C, et al. First-in-class thyrotropin-releasing hormone (TRH)-based compound binds to a pharmacologically distinct TRH receptor subtype in human brain and is effective in neurodegenerative models. Neuropharmacology. 2015;89:193–203.
4. Duval F, Mokrani M-C, Erb A, Danila V, Lopera FG, Foucher JR, et al. Thyroid axis activity and dopamine function in depression. Psychoneuroendocrinology. 2021;128: 105219.
5. Alvarez-Salas E, García-Luna C, de Gortari P. New efforts to demonstrate the successful use of TRH as a therapeutic agent. Int J Mol Sci. 2023;24:11047.
6. Jaworska-Feil L, Jantas D, Leskiewicz M, Budziszewska B, Kubera M, Basta-Kaim A, et al. Protective effects of TRH and its analogues against various cytotoxic agents in retinoic acid (RA)-differentiated human neuroblastoma SH-SY5Y cells. Neuropeptides. 2010;44:495–508.
7. Cantuti-Castelvetri I, Hernandez LF, Keller-McGandy CE, Kett LR, Landy A, Hollingsworth ZR, et al. Levodopa-induced dyskinesia is associated with increased thyrotropin releasing hormone in the dorsal striatum of hemi-parkinsonian rats. PLoS ONE. 2010;5: e13861.
8. Espadas I, Darmopil S, Vergaño-Vera E, Ortiz O, Oliva I, Vicario-Abejón C, et al. L-DOPA-induced increase in TH-immunoreactive striatal neurons in parkinsonian mice: Insights into regulation and function. Neurobiol Dis. 2012;48:271–81.
9. Muñoz-Manchado AB, Gonzales CB, Zeisel A, Munguba H, Bekkouche B, Skene NG, et al. Diversity of interneurons in the dorsal striatum revealed by single-cell RNA sequencing and PatchSeq. Cell Rep. 2018;24:2179-2190.e7.
10. Khomane KS, Meena CL, Jain R, Bansal AK. Novel thyrotropin-releasing hormone analogs: a patent review. Expert Opin Ther Pat. 2011;21:1673–91.
11. Yamamura M, Suzuki M, Matsumoto K. Synthesis and pharmacological action of TRH analog peptide(Taltirelin). Folia Pharmacologica Japonica. 1997;110:33–8.
12. Suzuki M, Sugano H, Matsumoto K, Yamamura M, Ishida R. Synthesis and central nervous system actions of thyrotropin-releasing hormone analogues containing a dihydroorotic acid moiety. J Med Chem. 1990;33:2130–7.
13. Brown WM. Taltirelin (Tanabe Seiyaku). IDrugs. 2001;4:1389–400.
14. Vijiaratnam N, Simuni T, Bandmann O, Morris HR, Foltynie T. Progress towards therapies for disease modification in Parkinson's disease. The Lancet Neurology. 2021;20:559–72.
15. Bloem BR, Okun MS, Klein C. Parkinson's disease. The Lancet. 2021;397:2284–303.
16. Surguchov A. Biomarkers in Parkinson's Disease. In: Peplow PV, Martinez B, Gennarelli TA, editors. Neurodegenerative Diseases Biomarkers: Towards Translating Research to Clinical Practice. Springer, US: New York NY; 2022. p. 155–80.
17. Burbulla LF, Song P, Mazzulli JR, Zampese E, Wong YC, Jeon S, et al. Dopamine oxidation mediates mitochondrial and lysosomal dysfunction in Parkinson's disease. Science. 2017;357:1255–61.
18. Calabresi P, Ghiglieri V, Mazzocchetti P, Corbelli I, Picconi B. Levodopa-induced plasticity: a double-edged sword in Parkinson's disease? Philos Trans R Soc Lond B Biol Sci. 2015;370:20140184.
19. Calabresi P, Di Filippo M, Ghiglieri V, Tambasco N, Picconi B. Levodopa-induced dyskinesias in patients with Parkinson's disease: filling the bench-to-bedside gap. Lancet Neurol. 2010;9:1106–17.
20. Zheng C, Chen G, Tan Y, Zeng W, Peng Q, Wang J, et al. TRH analog, taltirelin protects dopaminergic neurons from neurotoxicity of MPTP and rotenone. Front Cell Neurosci. 2018;12:485.
21. Zheng C, Chen G, Tan Y, Zeng W, Peng Q, Wang J, et al. TRH analog, taltirelin improves motor function of hemi-PD rats without inducing dyskinesia via sustained dopamine stimulating effect. Front Cell Neurosci. 2018;12:417.
22. Ijiro T, Yaguchi A, Yokoyama A, Kiguchi S. Rovatirelin ameliorates motor dysfunction in the cytosine arabinoside-induced rat model of spinocerebellar degeneration via acetylcholine and dopamine neurotransmission. Clin Exp Pharmacol Physiol. 2022;49:950–8.
23. Stanley G, Gokce O, Malenka RC, Südhof TC, Quake SR. Continuous and discrete neuron types of the adult murine striatum. Neuron. 2020;105:688-699.e8.
24. Xenias HS, Ibáñez-Sandoval O, Koós T, Tepper JM. Are striatal tyrosine hydroxylase interneurons dopaminergic? J Neurosci. 2015;35:6584–99.
25. Uchigashima M, Ohtsuka T, Kobayashi K, Watanabe M. Dopamine synapse is a neuroligin-2–mediated contact between dopaminergic presynaptic and GABAergic postsynaptic structures. Proc Natl Acad Sci USA. 2016;113:4206–11.
26. Li Z, Shang Z, Sun M, Jiang X, Tian Y, Yang L, et al. Transcription factor Sp9 is a negative regulator of D1-type MSN development. Cell Death Discov. 2022;8:1–12.
27. Gerfen CR, Engber TM, Mahan LC, Susel Z, Chase TN, Monsma FJ, et al. D1 and D2 dopamine receptor-regulated gene expression of striatonigral and striatopallidal neurons. Science. 1990;250:1429–32.
28. Morin N, Morissette M, Grégoire L, Di Paolo T. mGlu5, dopamine D $_2$ and adenosine A $_{2A}$ receptors in L-DOPA-induced dyskinesias. CN. 2016;14:481–93.
29. Puighermanal E, Castell L, Esteve-Codina A, Melser S, Kaganovsky K, Zussy C, et al. Functional and molecular heterogeneity of D2R neurons along dorsal ventral axis in the striatum. Nat Commun. 2020;11:1957.
30. Chen G, Nie S, Han C, Ma K, Xu Y, Zhang Z, et al. Antidyskinetic effects of MEK inhibitor are associated with multiple neurochemical alterations in the striatum of hemiparkinsonian rats. Front Neurosci. 2017. https://doi.org/10.3389/fnins.2017.00112.
31. Boldry RC, Papa SM, Kask AM, Chase TN. MK-801 reverses effects of chronic levodopa on D1 and D2 dopamine agonist-induced rotational behavior. Brain Res. 1995;692:259–64.
32. Pinna A, Pontis S, Borsini F, Morelli M. Adenosine A2A receptor antagonists improve deficits in initiation of movement and sensory motor

integration in the unilateral 6-hydroxydopamine rat model of Parkinson's disease. Synapse. 2007;61:606–14.
33. Chen Y, Chen Y, Shi C, Huang Z, Zhang Y, Li S, et al. SOAPnuke: a MapReduce acceleration-supported software for integrated quality control and preprocessing of high-throughput sequencing data. Gigascience. 2018;7:1–6.
34. Langmead B, Salzberg SL. Fast gapped-read alignment with Bowtie 2. Nat Methods. 2012;9:357–9.
35. Li B, Dewey CN. RSEM: accurate transcript quantification from RNA-Seq data with or without a reference genome. BMC Bioinformatics. 2011;12:323.
36. Wang L, Feng Z, Wang X, Wang X, Zhang X. DEGseq: an R package for identifying differentially expressed genes from RNA-seq data. Bioinformatics. 2010;26:136–8.
37. Samad TA, Krezel W, Chambon P, Borrelli E. Regulation of dopaminergic pathways by retinoids: activation of the D2 receptor promoter by members of the retinoic acid receptor–retinoid X receptor family. Proc Natl Acad Sci USA. 1997;94:14349–54.
38. Xicoy H, Wieringa B, Martens GJM. The SH-SY5Y cell line in Parkinson's disease research: a systematic review. Mol Neurodegeneration. 2017;12:10.
39. Fukuchi I, Asahi T, Kawashima K, Kawashima Y, Yamamura M, Matsuoka Y, et al. Effects of taltirelin hydrate (TA-0910), a novel thyrotropin-releasing hormone analog, on in vivo dopamine release and turnover in rat brain. Arzneimittelforschung. 1998;48:353–9.
40. Itoh Y, Yamazaki A, Ukai Y, Yoshikuni Y, Kimura K. Enhancement of brain noradrenaline and dopamine turnover by thyrotropin-releasing hormone and its analogue NS-3 in mice and rats. Pharmacol Toxicol. 1996;78:421–8.
41. Xu Y, Cai H, You C, He X, Yuan Q, Jiang H, et al. Structural insights into ligand binding and activation of the human thyrotropin-releasing hormone receptor. Cell Res. 2022;32:855–7.
42. Matre V, Karlsen HE, Wright MS, Lundell I, Fjeldheim AK, Gabrielsen OS, et al. Molecular cloning of a functional human thyrotropin-releasing hormone receptor. Biochem Biophys Res Commun. 1993;195:179–85.
43. Trubacova R, Drastichova Z, Novotny J. Biochemical and physiological insights into TRH receptor-mediated signaling. Front Cell Dev Biol. 2022;10: 981452.
44. Yin J, Chen K-YM, Clark MJ, Hijazi M, Kumari P, Bai X, et al. Structure of a D2 dopamine receptor-G protein complex in a lipid membrane. Nature. 2020;584:125–9.
45. Darmopil S, Muñetón-Gómez VC, de Ceballos ML, Bernson M, Moratalla R. Tyrosine hydroxylase cells appearing in the mouse striatum after dopamine denervation are likely to be projection neurones regulated by l-DOPA. Eur J Neurosci. 2008;27:580–92.
46. Arlotta P, Molyneaux BJ, Jabaudon D, Yoshida Y, Macklis JD. Ctip2 controls the differentiation of medium spiny neurons and the establishment of the cellular architecture of the striatum. J Neurosci. 2008;28:622–32.
47. Zhang X-R, Zhang Z-R, Chen S-Y, Wang W-W, Wang X-S, He J-C, et al. β-arrestin2 alleviates L-dopa-induced dyskinesia via lower D1R activity in Parkinson's rats. Aging (Albany NY). 2019;11:12315–27.
48. Gao S, Gao R, Yao L, Feng J, Liu W, Zhou Y, et al. Striatal D1 dopamine neuronal population dynamics in a rat model of levodopa-induced dyskinesia. Front Aging Neurosci. 2022;14: 783893.
49. Feyder M, Bonito-Oliva A, Fisone G. L-DOPA-induced dyskinesia and abnormal signaling in striatal medium spiny neurons: focus on dopamine d1 receptor-mediated transmission. Front Behav Neurosci. 2011;5:71.
50. Lee J, Gomez-Ramirez J, Johnston TH, Visanji N, Brotchie JM. Receptor-activity modifying protein 1 expression is increased in the striatum following repeated L-DOPA administration in a 6-hydroxydopamine lesioned rat model of Parkinson's disease. Synapse. 2008;62:310–3.
51. Darmopil S, Martín AB, Diego IRD, Ares S, Moratalla R. Genetic inactivation of dopamine D1 but not D2 receptors inhibits L-DOPA-induced dyskinesia and histone activation. Biolog Psychiatry. 2009. https://doi.org/10.1016/j.biopsych.2009.04.025.
52. Seeman P. Targeting the dopamine D2 receptor in schizophrenia. Expert Opin Ther Targets. 2006;10:515–31.
53. Fields AL, Soprano DR, Soprano KJ. Retinoids in biological control and cancer. J Cell Biochem. 2007;102:886–98.
54. Tang X-H, Gudas LJ. Retinoids, retinoic acid receptors, and cancer. Annu Rev Pathol Mech Dis. 2011;6:345–64.
55. Gudas LJ, Wagner JA. Retinoids regulate stem cell differentiation. J Cell Physiol. 2011;226:322–30.
56. McCaffery P, Dräger UC. High levels of a retinoic acid-generating dehydrogenase in the meso-telencephalic dopamine system. Proc Natl Acad Sci USA. 1994;91:7772–6.
57. Ransom J, Morgan PJ, McCaffery PJ, Stoney PN. The rhythm of retinoids in the brain. J Neurochem. 2014;129:366–76.
58. Jacobs FMJ, Smits SM, Noorlander CW, Von Oerthel L, Van Der Linden AJA, Burbach JPH, et al. Retinoic acid counteracts developmental defects in the substantia nigra caused by Pitx3 deficiency. Development. 2007;134:2673–84.
59. Podleśny-Drabiniok A, Sobska J, De Lera AR, Gołembiowska K, Kamińska K, Dollé P, et al. Distinct retinoic acid receptor (RAR) isotypes control differentiation of embryonal carcinoma cells to dopaminergic or striatopallidal medium spiny neurons. Sci Rep. 2017;7:13671.
60. Brignani S, Raj DDA, Schmidt ERE, Düdükcü Ö, Adolfs Y, De Ruiter AA, et al. Remotely produced and axon-derived netrin-1 instructs Gabaergic neuron migration and dopaminergic substantia Nigra development. Neuron. 2020;107:684-702.e9.
61. Kang EJ, Jang SM, Lee YJ, Jeong YJ, Kim YJ, Kang SS, et al. The couple of netrin-1/α-Synuclein regulates the survival of dopaminergic neurons via α-Synuclein disaggregation. BMB Rep. 2023;56:126–31.
62. Chen G, Ahn EH, Kang SS, Xia Y, Liu X, Zhang Z, et al. UNC5C receptor proteolytic cleavage by active AEP promotes dopaminergic neuronal degeneration in Parkinson's disease. Adv Sci (Weinh). 2022;9: e2103396.
63. Jasmin M, Ahn EH, Voutilainen MH, Fombonne J, Guix C, Viljakainen T, et al. Netrin-1 and its receptor DCC modulate survival and death of dopamine neurons and Parkinson's disease features. EMBO J. 2021;40: e105537.

Publisher's Note